INSTITUTE OF PHYSICS PUBLISHING JOURNAL OF PHYSICS: CONDENSED MATTER

J. Phys.: Condens. Matter **16** (2004) R83–R110 PII: S0953-8984(04)70229-5

TOPICAL REVIEW

Neutron scattering and molecular dynamics simulation: a conjugate approach to investigate the dynamics of electron transfer proteins

Anna Rita Bizzarri[1]

Biophysics and Nanoscience Group, INFM, Dipartimento di Scienze Ambientali, Universita' della Tuscia, I-01100 Viterbo, Italy

E-mail: bizzarri@unitus.it

Received 13 October 2003, in final form 19 December 2003
Published 30 January 2004
Online at stacks.iop.org/JPhysCM/16/R83 (DOI: 10.1088/0953-8984/16/6/R01)

Abstract

The neutron scattering technique is a relevant tool for studying the dynamical properties of electron transfer proteins. Macromolecular motions ranging in wide temporal and spatial windows can be investigated by separately analysing elastic, inelastic and quasielastic incoherent neutron scattering. The dynamical behaviour of the solvent surrounding a macromolecule can also be analysed. Neutron scattering is particularly rewarding when used in combination with molecular dynamics simulations. From the simulated atomic trajectories, physical quantities directly related to the neutron scattering technique can be calculated and compared with the corresponding experimental data. This article briefly introduces both the neutron scattering and molecular dynamics simulation methods applied to proteins, and reviews the biophysical studies of some electron transfer proteins. Both experimental and molecular dynamics results for these proteins and the surrounding solvent are also discussed in connection with their electron transfer properties. Possible developments are briefly outlined.

(Some figures in this article are in colour only in the electronic version)

Contents

[1] web site: www.unitus.it/biophysics

1. Introduction

Electron transfer (ET) is an integral part of many biological processes, mediated by a specific class of proteins, such as storage and energy consummation and photosynthesis. ET proteins carry or shuttle electrons between a donor and an acceptor [1, 2]. Although ET is inherently an electronic process, i.e. a transition between two electron states, it is facilitated by nuclear motions in the protein and the surrounding solvent [3]. In the framework of the Marcus theory, the environment degrees of freedom coupled to the ET reaction are divided into two groups [1]: the inner sphere coordinates which are intramolecular vibrational modes at the active site, and a single outer sphere classical collective coordinate, which describes the rearrangement of the remaining degrees of freedom. Accordingly, the overall protein dynamics contributes to determining and regulating the peculiar ET process occurring at the active site. Protein motions might yield a fine tuning of the ET process through a modulation of the structural parameters of the redox centre. Indeed, in ET copper proteins, small movements of protein residues near the reaction centre finely modulate the value of the redox potential of the ET reaction. Also movements of protein atoms far from the copper site could be relevant to allow the electron to travel a long distance from the docking site to the metal centre [3]. Conformational changes in proteins involve the vibrational normal modes of the macromolecule [4]. There are thousands of modes ranging from high frequency well-defined localized modes to very low frequency delocalized modes. In ET proteins, these delocalized, collective modes could regulate the partner recognition as well as the binding process [5, 6]; such a process being supported by the macromolecular structure, specifically tailored to perform and regulate the specific functional role.

Furthermore, the solvent dynamics, strictly coupled to the protein motions [7–9] can strongly affect the ET properties [3]. A threshold level of hydration of about 0.40 g of water/g of protein, approximatively corresponding to a layer of water at the protein surface, is at least required to fully activate the dynamics and functionality of globular proteins [10–13]. A full understanding of the protein dynamics as well as of its coupling to the solvent, represents an essential step to fully clarify the mechanisms operating within ET biomolecules.

ET proteins share with other biomolecules a very complex structure which is reflected in a huge variety of motions. Generally, several techniques such as x-ray diffraction [14], Mössbauer [15, 16], optical [17], Raman scattering [18, 19], magnetic resonance spectroscopies [20, 21], and neutron scattering [22, 23], preferentially at different

temperatures, have been applied to describe the dynamical behaviour of proteins; each technique providing information within a peculiar spatial and temporal window. Neutron scattering, by measuring the exchange of energy and momentum between the neutrons and the biomolecule sample, gives a description of protein motions in the pico- and nanosecond timescales, over lengths in the 0.1–100 Å region, probing both vibrational and diffusive motions.

Neutron scattering has two components: an incoherent one, which arises from self-correlations in atomic motions, and a coherent one which arises from self- and cross-correlation in the atomic positions [22]. Neutron scattering of proteins is generally dominated by the strong incoherent contribution from protons which, being uniformly distributed within the whole macromolecule, can monitor the overall protein dynamics. Isotopic contrast can be employed to improve neutron scattering results. By exploiting the large difference in the neutron scattering cross section of deuterium (D) and hydrogen (H) isotopes, the dynamical behaviour of the protein or that of the solvent can be singled out by analysing a protein hydrated with D_2O or a deuterated protein hydrated by H_2O [24]. However, the presence of exchangeable protein protons with variable exchanging times requires particular care in sample preparation as well in data analysis [25]. To maximize the neutron scattering signal, protein dynamics is usually studied in powder samples with a low water content (less than 0.5 g of water/g of protein); experiments on aqueous samples being recently performed [26].

Incoherent neutron scattering (INS) is usually separated into elastic, quasielastic and inelastic components; each one of these terms providing a different kind of information on protein dynamics [22, 27].

Elastic INS, related to the correlations in the atomic positions at infinite time, gives information on the geometry of motions [28]. From the elastic scattering, the mean square displacements (MSD) of atomic motions can be extracted [29–34].

Quasielastic INS scattering, arising from stochastic motions, is mainly sensitive to hydrogen diffusive motions and, in principle, it provides relaxation times and motion shapes at the molecular level [27]. The timescale range at which these dynamical events occur in proteins is very wide [31, 35–41].

Finally, inelastic INS gives information about the vibrational dynamics of protein atoms [29, 42, 43], providing also the vibrational density of states of the biomolecular system [28, 44].

INS becomes much more rewarding when used in connection with molecular dynamics (MD) simulation [43, 45–50]. Classical MD simulations give a detailed atomic, spatial and temporal description of both protein and solvent dynamics in the same temporal window of neutron scattering [51, 52]. From MD simulated trajectories, the INS quantities can be calculated and compared with the corresponding experimental values [28, 44]. Therefore, once the reliability of the simulation has been assessed, the MD simulation capabilities can be exploited to extract information which cannot be directly obtained from experimental data [28]. For example, the contribution arising from protein hydrogens belonging to different regions can be extracted from the total INS signal [53]. On the other hand, we remark that MD simulation can help to elucidate the hydrogen/deuterium exchange in neutron scattering data of protein systems.

Here, the results as obtained by INS conjugated with MD simulation on the dynamics of ET proteins are reviewed. In particular, we have focused our attention on two ET copper-containing proteins, azurin (AZ) and plastocyanin (PC), which are members of a family of proteins collectively described as blue-copper proteins [54]. The investigation of these proteins, widely studied by both neutron scattering and MD simulations [43, 53, 55–59], could be paradigmatic for the general understanding of ET proteins.

2. Materials and methods

2.1. Neutron scattering of proteins

The basic quantity measured by neutron scattering experiments with thermal neutrons is the double differential cross-section $\mathrm{d}^2\sigma/\mathrm{d}\Omega\,\mathrm{d}E$ which is the number of neutrons scattered per unit time into solid angle interval $[\Omega, \Omega + \mathrm{d}\Omega]$ and energy interval $[E, E + \mathrm{d}E]$, normalized to the flux of the incoming neutrons:

$$\frac{\mathrm{d}^2\sigma}{\mathrm{d}\Omega\,\mathrm{d}E} = N\frac{k}{k_0}S_{\mathrm{tot}}(\mathbf{q}, \nu) \tag{1}$$

where the quantity $S_{\mathrm{tot}}(\mathbf{q}, \nu)$ is the dynamic structure factor, or scattering function, N is the number of atoms, $\mathbf{q}$ is the exchanged momentum, ν is the frequency related to the exchange energy $h\nu$ and k and k_0 are the absolute values of the wavevectors of scattered and incident neutrons, respectively (see figure 2) [27]. The experimental data from some neutron equipments are sometimes reported as a function of the scattering angle θ, instead of $\mathbf{q}$; θ being related to $\mathbf{q}$ through the difference $\mathbf{k} - \mathbf{k_0}$ (see figure 2).

The dynamic structure factor contains information about the dynamics of the sample. It includes a coherent part, $S_{\mathrm{coh}}(\mathbf{q}, \nu)$, arising from interference effects due to correlations in the positions of different atoms, and an incoherent part, $S_{\mathrm{inc}}(\mathbf{q}, \nu)$, related to the self-correlation in the atomic positions [22]. The incoherent scattering of hydrogen atoms, which is an order of magnitude larger than those of the other atoms, dominates the spectra profiles of protein systems [22]. For protein systems, the coherent contribution to the total signal can be evaluated to be about 15–20% [59].

The incoherent dynamic structure factor may be written as the spatial-temporal Fourier transform of the self-correlation function, $g(\mathbf{r}, t)$, [22]:

$$S_{\mathrm{inc}}(\mathbf{q}, \nu) = \frac{1}{2\pi}\int_{-\infty}^{+\infty}\int_{-\infty}^{+\infty} g(\mathbf{r}, t)\mathrm{e}^{-2\pi\mathrm{i}\nu t}\mathrm{e}^{-\mathrm{i}\mathbf{q}\cdot\mathbf{r}}\,\mathrm{d}t\,\mathrm{d}\mathbf{r}, \tag{2}$$

the self-correlation function, $g(\mathbf{r}, t)$, or the Van Hove function, being given by [22]:

$$g(\mathbf{r}, t) = \frac{1}{N}\sum_{i=1}^{N}\langle\delta[\mathbf{r} + \mathbf{R}_i(0) - \mathbf{R}_i(t)]\rangle \tag{3}$$

where the sum is performed over the number N of hydrogens in the system, $\mathbf{r}$ is a position vector, $\mathbf{R}_i(t)$ is the position vector of the ith hydrogen at time t and the brackets $\langle\,\rangle$ denote an average over time origins.

In practice, the spread in energy of the neutrons incident on the sample results in a finite energy resolution and the measured spectrum, $S_{\mathrm{inc}}^{\mathrm{exp}}(\mathbf{q}, \nu)$, is a convolution of the true spectrum $S_{\mathrm{inc}}(\mathbf{q}, \nu)$ with the instrumental resolution function $R(\nu)$:

$$S_{\mathrm{inc}}^{\mathrm{exp}}(\mathbf{q}, \nu) = S_{\mathrm{inc}}(\mathbf{q}, \nu) \otimes R(\nu) \tag{4}$$

where $\otimes$ denotes a convolution product.

In the one-phonon scattering approximation [22], the incoherent dynamics structure factor is usually written as the sum of three terms:

$$S_{\mathrm{inc}}(\mathbf{q}, \nu) = \mathrm{e}^{-2W(q,T)}A_0(\mathbf{q}) \cdot \delta(\nu) + \mathrm{e}^{-2W(q,T)}[1 - A_0(\mathbf{q})] \cdot S_{\mathrm{qel}}(\mathbf{q}, \nu) + S_{\mathrm{inel}}(\mathbf{q}, \nu) \tag{5}$$

where $\mathrm{e}^{-2W(q,T)}$ is the Debye–Waller factor, $A_0(\mathbf{q})$ is the elastic incoherent structure factor, $\delta(\nu)$ is the delta function, $S_{\mathrm{qel}}(\mathbf{q}, \nu)$ is the quasielastic incoherent structure factor and $S_{\mathrm{inel}}(\mathbf{q}, \nu)$ is the inelastic incoherent structure factor.

The first term in equation (5), giving the elastic response of the system $S_{\mathrm{el}}(q, \nu \approx 0)$, can be obtained as the limit of INS function for infinite time [22]. In the Gaussian approximation,

the elastic dependence on the energy is represented by a delta function and the Debye–Waller factor can be expressed by:

$$e^{-2W(q,T)} = e^{-q^2\langle u(T)^2\rangle/6} \tag{6}$$

where $\langle u^2(T)\rangle$ is the averaged hydrogen MSD at temperature T. Accordingly, the MSD of hydrogen atoms can be estimated by extracting the limiting slope as $\mathbf{q} \to 0$ of $\ln S_{\mathrm{inc}}(q, \nu = 0)$ versus q^2 at various temperatures [29]; such a quantity being dependent on the energy resolution of the instrument. Alternatively, to take into account the variety of protein motions, the MSD can be extracted from the relationship:

$$\langle u^2(T)\rangle = \int \langle u^2(T)\rangle g(\langle u^2(T)\rangle)\, \mathrm{d}\langle u^2(T)\rangle \tag{7}$$

where $g(\langle u^2(T)\rangle)$ is the probability distribution function corresponding to motions characterized by $\langle u^2(T)\rangle$; the integration in equation (7) being carried out on the whole domain of motions resolvable by the instrument used. It should be remarked that the MSD obtainable from neutron scattering should be distinguished from the mean square fluctuation as obtained from x-ray crystallography [28]. Actually, the former gives information about a deviation of the protein from a reference structure in the temporal window of the neutron scattering measurements; the latter providing time-averaged information about the mobility of protein atoms by considering the static disorder (crystal disorder and structural macromolecular heterogeneity) [60].

The inelastic INS scattering consists of peaks at non-zero values of the energy transfer. For proteins, the inelastic contribution results from an exchange of energy with vibrational modes in the molecule and it can be expressed by:

$$S_{\mathrm{inel}}(\mathbf{q}, \nu) = e^{-2W(q,T)} \frac{q^2}{8\pi M \nu} n(\nu, T) g(\nu) \tag{8}$$

where M is the proton mass, $n(\nu, T) = [e^{h\nu/k_B T} - 1]^{-1}$ is the Bose factor and $g(\nu)$ is the vibrational density of states.

From neutron scattering data, the amplitude-weighted vibrational density of states, $G(\nu)$, can be obtained by taking the limit $q \to 0$ [42, 46]:

$$G(\nu) = \lim_{q\to 0} \frac{6\nu}{hq^2} (e^{h\nu/kT} - 1) S_{\mathrm{inc}}(q, \nu) \tag{9}$$

such a function $G(\nu)$ practically coincides with the density of states $g(\nu)$ in the low frequency region [42].

Finally, the quasielastic INS, $S_{\mathrm{qel}}(q, \nu)$, which appears by increasing the temperature, gives rise to a broadening of the elastic peak; such a broadening being due to stochastic motions and overdamped vibrational modes. To extract the quasielastic contribution, a subtraction of the inelastic scattering from the total INS spectrum is usually performed. Under the assumption that harmonic and anharmonic motions are statistically independent [42], the quasielastic contribution at the temperature T can be estimated by a careful subtraction of the vibrational part from the total spectrum:

$$S_{\mathrm{qel}}(q, \nu, T) = S_{\mathrm{inc}}(q, \nu, T) - S_{\mathrm{inel}}(q, \nu, T). \tag{10}$$

In the hypothesis that at the low temperature T_0, protein dynamics follows a harmonic behaviour, low temperature spectra at T_0 can be used to approximate the vibrational component at higher temperature T through:

$$S_{\mathrm{inel}}(q, \nu, T) = S_{\mathrm{inc}}(q, \nu, T_0) \frac{e^{-2W(q,T)n(\nu,T)}}{e^{-2W(q,T_0)n(\nu,T_0)}}. \tag{11}$$

For simple homogeneous systems, the quasielastic contribution is commonly represented by a Lorentzian centred at $\nu = 0$. For proteins, the quasielastic scattering, which results from very complex diffusive atomic motions, is quite difficult to extract. A phenomenological function, such as a sum of Lorentzians is frequently proposed to describe the quasielastic INS:

$$[1 - A_0(q)]S_{\mathrm{qel}}(q, \nu) = \sum QISF_n(q)L_n(\sigma_n, \nu) \tag{12}$$

where $L_n(\sigma_n, \nu)$ is the nth Lorentzian, σ_n is the full width at half-maximum, the inverse of which provides an estimation of the characteristic timescale of the corresponding motion and $QISF_n(q)$ is the quasielastic incoherent structure factor which gives the energy integral of the nth quasielastic component.

2.2. Hydrogen/deuterium exchange in proteins

As already mentioned, the neutron scattering of a protein system is largely dominated by the scattering of hydrogens which are evenly distributed in the protein macromolecule and, if present, in the surrounding water. By taking into account that the incoherent cross-section of hydrogens is 80×10^{-24} cm^{-2} and that of deuterium is 2×10^{-24} cm^{-2}, the H/D contrast can be exploited in INS experiments to selectively enhance the dynamics of a part of the system. Indeed, to maximize the contribution due to protein motions, INS experiments are performed in a D_2O medium. However, the presence of exchangeable protein hydrogens, with different exchanging times, gives rise to a continuous exchange between the protein and the solvent hydrogens [59, 61, 62]. To substitute all the rapidly exchanging protein H by D atoms, a protein can be dissolved in D_2O, then it can be lyophilized and hydrated again with D_2O. On the other hand, to substitute by deuterium all the protein exchangeable protons, even those with a large exchanging rate, a protein can be dissolved in bulk D_2O and left for a long period. Then it can be lyophilized, and solved again in D_2O by repeating such a procedure a number of times. Furthermore, since the large majority of exchangeable hydrogens is generally located on the protein surface, by appropriately using D-labelling, the dynamics of exposed or core protein residues can be selectively highlighted [59, 63, 64].

Conversely, the dynamical behaviour of the solvent can be obtained from INS data by following two different strategies. First, a quantitative comparison between INS data from a protein system alternatively hydrated by H_2O or D_2O can be performed. A second approach consists in growing the protein in deuterated media [65] and then hydrating it by H_2O; such a procedure allowing the direct extraction of the solvent contribution [66, 38]. However, again, the presence of the hydrogen exchanging processes between the protein and the solvent requires some care in the analysis of the results [56].

2.3. MD simulation of proteins and derivation of neutron scattering quantities

The classical dynamics of a protein system can be simulated, at atomic resolution, by integrating the Newton equations for each atom; such an approach involving the computation of the coordinates and velocities of each atom in the system as a function of time. The essential prerequisites are the knowledge of a starting set of atomic coordinates (for proteins usually obtained from x-ray crystallographic or refined-NMR structure data) and of the interaction potential among atoms. Usually, the interaction potential is represented by an empirical energy function that takes into account both the bonding and the non-bonding contributions [51, 52, 67]:

$$U(\mathbf{R}) = \tfrac{1}{2}\sum_{\text{bonds}} K_{\mathrm{b}}(b-b_0)^2 + \tfrac{1}{2}\sum_{\text{angle}} K_\theta(\theta-\theta_0)^2 + \tfrac{1}{2}\sum_{\text{dihedrals}} K_\chi[1+\cos(n\chi-\delta)] + \tfrac{1}{2}\sum_{\text{impropers}} K_{\mathrm{imp}}(\phi-\phi_0)^2 + \sum_{\text{non-bondedpairs}} \epsilon_{ij}\left[\left(\frac{\sigma_{ij}}{r_{ij}}\right)^{12} - \left(\frac{\sigma_{ij}}{r_{ij}}\right)^{6}\right] + \frac{q_i q_j}{4\pi\epsilon_0 r_{ij}} \tag{13}$$

where $\mathbf{R}$ is the coordinates of the atoms, K_{b}, K_θ, $K_\chi K_{\mathrm{imp}}$ are the bond, angle, dihedral angle an improper dihedral angle force constants, respectively, b, θ, χ, ϕ are the bond length, bond angle, dihedral angle and improper torsion angle, respectively, and the subscript zero represents the equilibrium values for the individual terms. Lennard-Jones 6–12 and Coulomb terms contribute to the external or non-bonded interactions; ϵ_{ij} is the Lennard-Jones well depth and σ_{ij} is the distance at the Lennard-Jones minimum between atoms i and j, q_i is the partial atomic charge, ϵ_0 is the dielectric constant, and r_{ij} is the distance between atoms i and j. Different sets of parameters for the empirical potential energy function have been developed (CHARMM, GROMOS, AMBER, ENCAD) [68–71]. At the same time, a variety of potential functions to describe intermolecular liquid water interactions have been proposed and tested (SPC [72], SPC/E [73], TIP3P [74], F3C [75], ST2 [76]).

The macromolecule can be partially hydrated by a layer of water molecules just covering the solvent-exposed surface or it can be fully solvated by a large box filled with solvent molecules. In the last case, the whole system is usually replicated in three dimensions and treated with periodic boundary conditions [77]. To save computational time, a variety of approximate methods for the treatment of electrostatic long range interactions have been developed [77–81]. Given an initial set of atomic coordinates and velocities, a numerical integration of equations of motions is performed [82] by keeping constant the energy constant (microcanonical or NVE ensemble), the temperature (canonical or NVT ensemble) or both pressure and temperature constant (isobaric–isothermal or NPT ensemble) [77].

The stored MD simulated trajectories of protein atoms can be exploited to calculate some relevant physical quantities which are directly connected to INS parameters.

The self-intermediate incoherent scattering function $I_{\mathrm{inc}}(q,t)$ can be derived from MD simulation through the expression:

$$I_{\mathrm{inc}}(q,t) = 1/3N\left\langle \sum_{i=1}^{N} \mathrm{e}^{[\mathrm{i}\mathbf{q}\cdot(\mathbf{R}_i(t)-\mathbf{R}_i(0))]} \right\rangle \tag{14}$$

where $\mathbf{R}_i(t)$ is the position vector of the ith atom at time t, and the brackets $\langle\,\rangle$ denote an averaging over the system atoms, the time origin and, to take into account anisotropic effects, the exchange momenta $\mathbf{q}$ having the same modulus q.

The incoherent dynamic structure factor $S_{\mathrm{inc}}(q,\nu)$ can be calculated by the temporal Fourier transform of $I_{\mathrm{inc}}(q,t)$:

$$S_{\mathrm{inc}}(q,\nu) = \frac{1}{2\pi}\int_{-\infty}^{+\infty} \mathrm{e}^{(-2\mathrm{i}\pi\nu t)} I_{\mathrm{inc}}(q,t)\,\mathrm{d}t \tag{15}$$

which is usually derived by applying a numerical fast Fourier transform, also by convoluting $S_{\mathrm{inc}}(q,\nu)$ with a function to take into account the experimental resolution. In addition, to satisfy the detailed balance condition, a semiclassical correction is applied by multiplying $S_{\mathrm{inc}}(q,\nu)$ by the factor $\exp(h\nu/2k_{\mathrm{B}}T)$ [44].

Under the assumption that the short time behaviour of protein atoms can be described as independent harmonic oscillators (oscillatory motion in the cage formed by its neighbours), the vibrational density of states $g(\nu)$ can be derived from MD simulated trajectories by different

approaches. It can be obtained from the spectral density $C_{vv}(\nu)$ of the velocity autocorrelation function $C_{vv}(t)$ [55]:

$$g(\nu) \sim C_{vv}(\nu) = \frac{1}{2\pi} \int_{-\infty}^{\infty} \mathrm{e}^{-2\pi \mathrm{i}\nu t} C_{vv}(t)\, \mathrm{d}t \tag{16}$$

with $C_{vv}(t)$ is expressed by:

$$C_{vv}(t) = \frac{1}{N} \sum_{i=1}^{N} \frac{1}{t_{\mathrm{run}} - t} \int_{0}^{T_{\mathrm{c}}} \mathbf{v}_i \cdot (t+\tau)\mathbf{v}_i(\tau)\, \mathrm{d}\tau \tag{17}$$

where $\mathbf{v}_i(t)$ is the velocity of the protein atom i at time t and t_{run} is the total time interval; $C_{vv}(t)$ being usually multiplied by a Gaussian damping envelope to overcome spurious truncation effects. Alternatively, the vibrational density of states $g(\nu)$ can be obtained by normal mode analysis (NMA) [83].

The MSD, $\langle u_i^2 \rangle$, of the ith atom can be derived from the MD trajectories through the relationship:

$$\langle u_i^2 \rangle = \langle (\mathbf{R}_i(t) - \mathbf{R}_i(0))^2 \rangle \tag{18}$$

by calculating the differences between the instantaneous, $\mathbf{R}_i(t)$ and averaged $\langle \mathbf{R}_i \rangle$ coordinates of ith atom; the brackets $\langle\ \rangle$ representing a time average.

Finally, to extract the quasielastic contribution, by analogy with the procedure used for the experimental data, a subtraction of the inelastic scattering from the total MD simulated INS dynamic structure factor is performed (see equations (10) and (11)).

2.4. Electron transfer proteins: azurin and plastocyanin

AZ and PC are copper containing proteins which play a crucial role in acting as ET agents in redox [84] and photosynthetic systems, respectively [85]. Both proteins consist of a rigid core formed by eight stranded β-strands, arranged in a β-sandwich, connected by random chains (turns) and of an α helical insertion [86, 87]. AZ contains a disulphide bridge connecting two β-strands [87] (see figure 1). The AZ and PC copper reaction sites are at one end of the β-sandwich structures. The geometry of the PC copper site is described as a distorted tetrahedral arrangement of three strongly bound ligands (two histidine and one cysteine) and one more weakly bound ligand (methionine) around the copper [86]. The AZ copper site has been found to share the same four ligands in a similar geometry, but with the possibility of a weak fifth ligand [87].

The PC protein surface, which represents the barrier through which the electron has to enter in an ET event, is characterized by a pronounced negative patch and a flat hydrophobic patch around the partly solvent exposed Cu-ligand His87 [85, 84]; such patches being found to be involved in the binding interaction with cytochrome f and Photosystem I [85, 84]. Similarly, on the AZ surface, a large hydrophobic patch located around the Cu-ligand His117 has been suggested as a likely candidate for reaction of AZ with both nitrite reductase and cytochrome c_{551} [88].

Both these proteins shuttle an electron from the donor to the acceptor involving the copper active site. Many studies have demonstrated that the ET process in AZ and PC is strongly regulated by their global structure and dynamics [89]. Indeed, even atoms far from the active site assist the ET process by determining and regulating the ET paths from the copper to the relative partners [6]. Collective motions, whose presence has been verified in ET proteins, form part of the reaction coordinates of the functional motions [6].

The reliability of the force field, used in the MD simulations of these proteins and of their active sites, has been also assessed by analysing the power spectrum as extracted from the

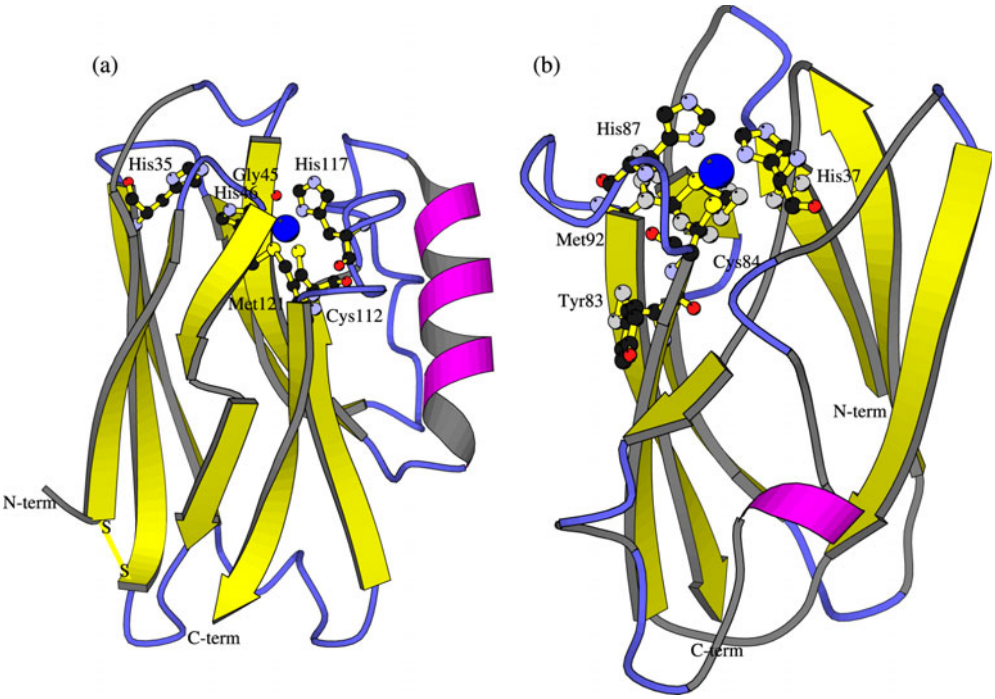

Figure 1. X-ray structures of AZ and PC. The copper atom (large dark sphere) and its ligands together with the N- and C-terms of the macromolecules are shown. These drawings have been generated using the program Molscript [145].

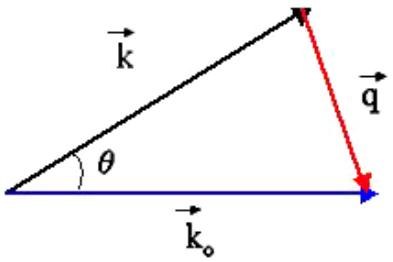

Figure 2. Scattering triangle of a neutron scattering event. $\mathbf{k_0}$ and $\mathbf{k}$ are the incident and the emerging scattering wavevectors, respectively. $\mathbf{q}$ is the exchanged momentum and θ is the scattering angle.

temporal fluctuations of the S–Cu bond distance during the temporal evolution [90]. Actually, such a spectrum has been shown to be very similar to that obtained by resonant Raman spectroscopy [91].

3. Incoherent neutron scattering and MD simulation results

3.1. Experimental dynamic structure factor

An example of the experimental dynamic structure factor, in θ representation, of D_2O hydrated and dry AZ powder samples, at different temperatures 100, 180, 220 and 300 K, is shown in

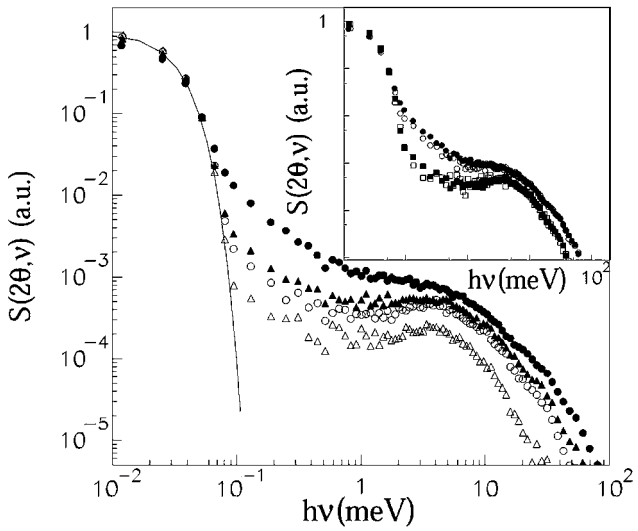

Figure 3. Experimental dynamic structure factor, $S(2\theta, \nu)$, as a function of $h\nu$, of a D_2O hydrated AZ powder sample (0.36 g of D_2O/g of protein) at $2\theta = 105°$ for different temperatures: 100 K (open triangles), 180 K (open circles), 220 K (full triangle)s and 300 K (full circles). Inset: comparison between spectra of D_2O hydrated AZ (full symbols) and dry AZ (open symbols) at 180 K (squares) and 300 K (circles). Adapted from [43].

figure 3. On visual inspection, the $S(2\theta, \nu)$ trend appears quite similar to that of other globular proteins [92, 43]. Each spectrum may be considered as the sum of three different contributions, i.e. the elastic, quasielastic and inelastic as described in section 2.1. The elastic peak is not a delta function but has a well defined linewidth because of the finite experimental resolution (represented by the dashed curve in figure 3); such a linewidth corresponding to the limit of the slowest observable motions. The elastic intensity decreases upon increasing the temperature, according to the Debye–Waller factor behaviour (see equation (6)), and such a decrease is compensated for by quasielastic and inelastic scattering.

The low-frequency inelastic spectra show a well-defined excess intensity around 3.5 meV, particularly visible at low temperatures. As the temperature increases, such a peak becomes less distinguishable, due to the rise of the quasielastic contribution which gradually fills up the low-temperature minimum.

The dynamic structure factor of the dry AZ sample at 180 and 300 K, shown in the inset of figure 3 together with the spectra from the corresponding hydrated sample, exhibits a quite similar behaviour to that of the hydrated sample. At 180 K a slight downwards shift of the inelastic peak is observed in the dry sample with respect to the hydrated one, while at room temperature the quasielastic contribution of the dry sample is slightly lower than the hydrated one.

Information about the overall protein dynamics contained in the experimental dynamic structure factor is analysed in more detail in the following. In particular, the different parts of the dynamic structure factor of AZ and of PC are separately addressed and compared with the related quantities as extracted from MD simulations.

3.2. Elastic incoherent neutron scattering intensity and mean square displacements

Figure 4 shows the normalized elastic intensity of dry and D_2O hydrated AZ samples as a function of temperature. The trend of dry AZ is characterized by a harmonic behaviour over all

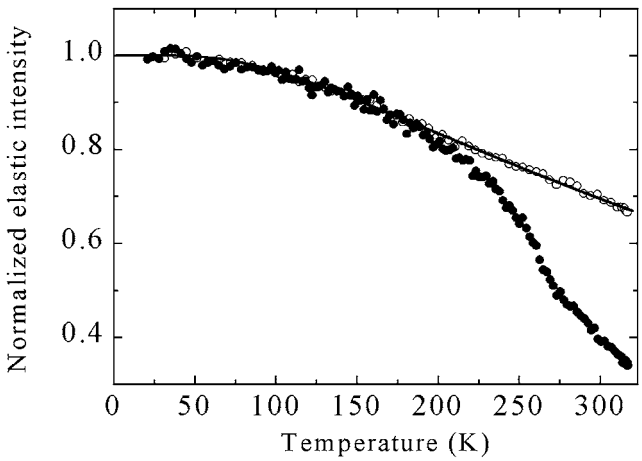

Figure 4. Experimental neutron scattering elastic intensity, as a function of temperature of D_2O hydrated (0.36 g of D_2O/g of protein) (full symbols) and dry (open symbols) AZ samples. The continuous curve shows a fit by a harmonic model. The data have been normalized to the elastic intensity at 20 K.

the analysed temperatures (see the continuous curve in figure 4). A similar behaviour is detected for D_2O hydrated AZ below 180 K. At variance, above this temperature, hydrated AZ reveals a drastic decrease in the elastic intensity, indicative of an anharmonic behaviour [93]; such a transition reflecting the onset of additional degrees of freedom. This finds a correspondence with what is observed in other protein systems [29, 32]. It is worth noting that the transition temperature varies with the energy resolution of the instrument used; the resolution directly reflecting the shortest detectable motions. Therefore, the observed dynamical transition involves protein motions with different characteristic times. For AZ, the transition temperature has been observed in a range from 180 to 230 K, corresponding to the onset of motions with characteristic times ranging from about 50 to 500 ps [94].

From figure 4, in addition to the transition at 230 K, a further change in the slope of the elastic intensity of hydrated AZ can be revealed at about 260 K, reflecting the onset of a new dynamical regime [94]. Since such a deviation can be put into evidence only by instruments detecting motions whose characteristic times are above 500 ps [94], it becomes apparent that, at higher temperatures, slower protein motions are established.

Further information about protein motions can be obtained from the MSD. The MSD of D_2O hydrated AZ, as extracted from the elastic intensity by integrating over all the accessible motions from 0.08 to 25 Å (see equation (7)), are shown, as a function of temperature, in figure 5; the probability distribution function, $g(\langle u^2(T)\rangle)$, having been estimated by the Monte Carlo method [93]. For temperatures below about 180 K, the MSD increases linearly with temperature as expected for harmonic motions (see continuous line in figure 5). Above this temperature, an extra increase in the MSD can be observed; such a trend reflecting the onset of anharmonic motions. A similar qualitative behaviour can be also observed in the inset of figure 5 where the MSD of D_2O hydrated AZ, as extracted from the limiting slope for $q \to 0$ of the dynamic structure factor (see section 2.1), are shown. Additionally, in the inset of figure 5, the MSD values at 180 and 300 K for the dry AZ sample suggest a harmonic behaviour according to what is observed in the elastic intensity. Generally, these results are in agreement with those found for other dry proteins [30, 31].

Notably, the MSD values, as obtained by an integration over a larger domain of accessible motions, appear to be lower with respect to those derived by only considering motions at a fixed

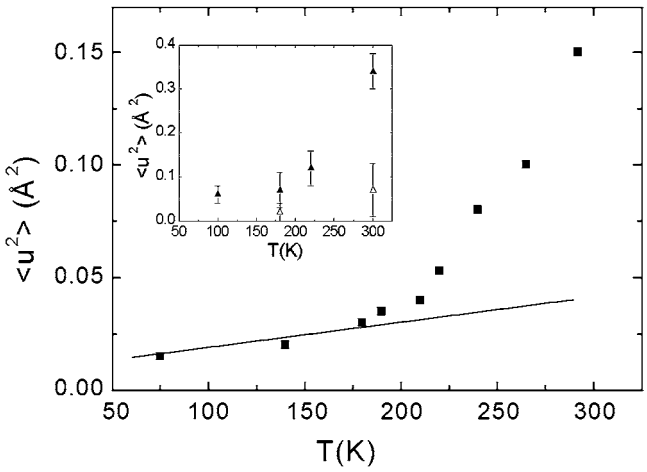

Figure 5. MSD, $\langle u^2 \rangle$, as a function of temperature, extracted through equation (7) from the experimental neutron scattering elastic intensity, of a D_2O hydrated (0.36 g of D_2O/g of protein) AZ sample. The continuous line shows a linear fit of the MSD values below 180 K. Inset: MSD, extracted from the limiting slope as $\mathbf{q} \to 0$, of $\ln S_{\rm inc}(q, \nu = 0)$ versus q^2 of D_2O hydrated (full triangles) and dry (open triangles) AZ samples. Adapted from [43, 93].

temporal resolution. Such a result, on the one hand suggests the presence of protein motions with a different amplitude and with different characteristic times, on the other it points out that motions with large amplitude give a smaller contribution to the MSD values [93].

From a general point of view, the deviation from the harmonic behaviour in the MSD as well as in the elastic intensity, around 200 K, might reflect the occurrence of a dynamical transition. Such a transition is commonly detected in hydrated proteins by several experimental investigations [29–32, 95–97] and it is quite similar to that observed in some glass-forming systems [98]. It has been suggested to be a sort of universal feature of protein systems likely due to the activation of transitions among different conformational substates, local minima of the proteins energy landscape [99, 100]. However, the existence of such a dynamical transition in proteins has been questioned due to its significant dependence on the timescale of the experimental accessible motions [101]. On such grounds, a discontinuity in the protein dynamics might not be required to explain the observed changes in the MSD slope as a function of temperature [101]. Irrespective of its origin, the evidence that the dynamical transition of proteins is almost suppressed in the dry samples is consistent with the hypothesis that the solvent plays a crucial role in regulating the dynamical response of a protein [102–104, 61, 105, 58, 8] (see also next section).

Recently, the investigation of the dynamical transition in proteins in the sub-nanosecond timescale by NMR has provided a new insight into the dynamics of proteins. Indeed, the observed protein transition at 200 K has been ascribed to a temperature activation of the methyl-side chain dynamics [106]; such activation being also strongly coupled to the solvent dynamics.

Finally, the slope change observed at about 260 K in the elastic scan of hydrated AZ reflects the onset, at higher temperature, of slower protein motions and appear quite striking. It could be consistent with the activation of a dynamical regime in which large parts of the macromolecule can be involved [107]. These slow motions might require the simultaneous collective arrangement of several residues and could be triggered by fast dynamical processes. This can be interpreted in the framework of a theory describing the dynamics of complex systems in terms of fast local motions as a precursor to slow collective motions [108, 29].

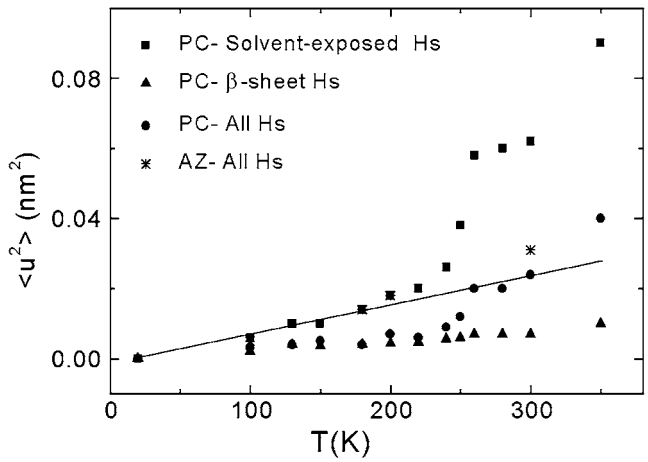

Figure 6. MD simulated MSD, $\langle u^2 \rangle$, as a function of temperature, of hydrated PC (0.40 g of D_2O/g of protein): all hydrogens (squares), solvent exposed hydrogens (triangles) and β-sheet hydrogens (circles). The continuous line shows a linear fit of the MSD values below 180 K for all hydrogens. The stars show the MD simulated MSD of hydrated AZ (0.40 g of D_2O/g of protein) at 100, 180, 220 and 300 K. Adapted from [110, 43].

From the biological point of view, the dynamical transition in proteins has been suggested to be related to the onset of the biological activity by involving an increase of the macromolecular flexibility [30, 35, 105, 109]. However, examples of protein systems which maintain their functionality even at low temperatures have been found [101]; such a finding supporting the hypothesis that some sort of uncorrelation between the biological activity and the onset of motions in the picoseconds timescale [101].

Finally, the fact that ET proteins behave similarly to other globular proteins provides support for the hypothesis that the global dynamical behaviour could be a common feature of proteins, irrespective of their specific function. Even proteins characterized by a quite rigid structure, like a β-barrel, may undergo a significant change, with temperature, in their dynamics.

3.3. MD simulated mean square displacements

Figure 6 shows the MSD, as a function of temperature, of hydrogen atoms for a hydrated PC sample as extracted from MD simulation in a temporal window of 500 ps. These MSD values appear to vary linearly with temperature below 180 K, while they increase more rapidly above 180 K; a similar trend being observed for the MSD of D_2O hydrated AZ at 100, 180, 220 and 300 K (see stars in figure 6). Therefore, the MD simulated MSD of both PC and AZ turn out to be consistent with the behaviour as observed in the INS experiments. However, we note that the MSD values from MD simulations should be re-scaled by a factor 0.4 in order to exactly match the experimental values. A similar quantitative discrepancy between the experimental and the MD computed MSD has been already observed in other hydrated proteins even if simulated by other potentials [45]. Such a behaviour may originate from a too soft MD force field which could lead to an overestimate of the atomic fluctuations [55]. In this respect, an effect due to the truncation of the long range electrostatic interactions could also be accounted for [47].

By exploiting the MD simulation capabilities, the contribution to the MSD arising from different PC classes of atoms can then be extracted. Figure 6 also shows the MD simulated

MSD for β-sheet hydrogens and solvent exposed side-chain hydrogens of PC. At all the temperatures, the solvent-exposed atoms are characterized by MSD values larger in comparison to those of β-sheet hydrogens. The prevailing location of the latter at the solvent accessible surface of the protein probably favours a large atomic mobility, while the motion of the β-sheet atoms is instead restrained by the rigid arrangement of the β-sandwich skeleton of the protein architecture. For dry PC [110], all the three atom classes behave harmonically below a temperature of about 130 K, after which the onset of an anharmonic contribution, less marked than in the hydrated PC system, occurs. All these results are in a qualitative agreement with the MD simulations of myoglobin at different levels of hydration [45].

As already mentioned, it is commonly believed that the solvent plays a crucial role in determining the dynamical transition of proteins. Actually, it has been shown that the dynamical transition of an hydrated protein can be inhibited by keeping only the solvent temperature below the glass-transition temperature [111]. Accordingly, the enhancement in the protein fluctuations magnitude above the glass-transition temperature can be assumed to be mainly due to the solvent mobility [112]. Further evidence for the intimate connection between protein and hydration water dynamics comes from the number of different water molecules engaged in the protein–solvent H-bonds for hydration water around PC [110, 113],whose trend with temperature is very similar to that observed in the protein MSD.

These findings have led some authors to hypothesize a strong coupling between the protein and the solvent dynamics [114, 110, 32, 115]. Hydration water dynamics could be coupled to the motion of the polar lateral chains through the injection of fast excitations which can trigger slower collective motions [114]. A discontinuity in length of the protein–solvent H-bond as a function of temperature, as detected by neutron scattering, [35, 116] could be at the origin of the onset of anharmonic protein motions at high temperature.

It should be mentioned that an analysis of the fluctuations in the MD simulated potential energy has revealed that both the PC and its surrounding solvent exhibit a $1/f^{\alpha}$ noise with the same value for the α exponent [117]. The presence of $1/f^{\alpha}$ noise, which is a manifestation, in the temporal domain, of the complexity of the system, could be put into relationship to the exploration of the complex energy landscape [118, 119]. The observed behaviour in the potential energy of PC, could, on one the hand be indicative of the complexity of the protein systems, on the other it could provide further evidence for the protein–solvent dynamical coupling.

3.4. Inelastic incoherent neutron scattering

The experimental dynamic structure factor, $S(\mathbf{q}, \nu)$, of D_2O hydrated AZ is shown in figure 7 for four different temperatures (100, 180, 220 and 300 K) at $q = 1.8$ Å^{-1}. As already mentioned, a broad low-frequency inelastic band centred around approximately 3.5 meV is well visible at low temperatures up to 220 K, but merges into the quasielastic contribution at room temperature. Generally such a peak, usually called boson peak, represents an excess of vibrational states over the flat Debye level. Indeed, in the Debye approximation and at low frequency, $g(\nu)$ turns out to be proportional to ν^2 and the Bose factor $n(\nu, T) = [e^{(h\nu/k_BT)} - 1]^{-1}$ can be cast in the form $k_BT/h\nu$; accordingly, a constant trend as a function of frequency is expected for the dynamic structure factor (see equation (8)). The presence of the boson peak in hydrated AZ can also be put into evidence as an excess of low-frequency modes in $g(\nu)$ [98]. Actually, in the inset of figure 7, the ratio $g(\nu)/\nu^2$ is shown for the different analysed temperatures, again revealing the presence of a bump located at about 3.5 meV for 100, 180 and 220 K. In addition, the density of low-frequency vibrations increases with the temperature and the maximum of $g(\nu)/\nu^2$ is shifting to lower energies.

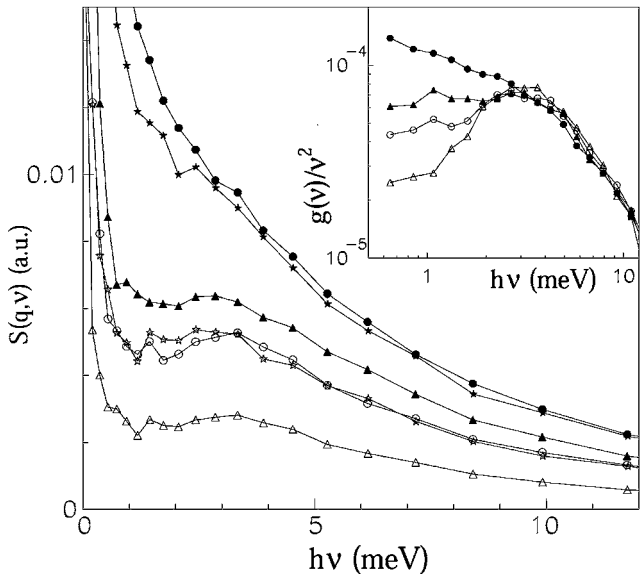

Figure 7. Experimental neutron scattering dynamic structure factor, $S(q, \nu)$, as a function of $h\nu$, at $q = 1.8$ Å^{-1}, of D_2O hydrated AZ (0.36 g of D_2O/g of protein) at different temperatures: 100 K (open triangles), 180 K (open circles), 220 K (full triangles) and 300 K (full circles) and of dry AZ at 180 K (open stars) and 300 K (full stars). Inset: vibrational density of states divided by ν^2, as a function of energy, of D_2O hydrated AZ at the same temperatures. Adapted from [43].

Figure 7 shows also the spectra for the dry AZ sample (stars) at 180 and at 300 K. The inelastic peak can also be seen at 180 K, but peaking at about 2.5–3 meV, slightly downwards shifted with respect to the corresponding hydrated sample in agreement with the results found for myoglobin [92].

The presence of an excess of scattering located at approximately the same range of 2–3.5 meV, has been seen in the low-temperature INS spectra, as well as in the Raman spectra at room temperature, of several proteins at different hydration conditions [28, 30, 42, 92, 120–124].

To better investigate the contribution of protein protons belonging to different classes, protein samples hydrated by D_2O and submitted to different hydrogen/deuterium exchange procedures can be analysed. Figure 8 shows the dynamic structure factor, at 100 K, of D_2O hydrated PC samples in which rapidly exchanging protons (open circles) and both rapidly and slowly exchanging protons (full circles) have been substituted by deuterium (for the hydrogen/deuterium exchange procedure see section 2). A bump at 3.5 meV is present in the dynamic structure factor of both the samples in agreement with what is observed for AZ [59] (for additional data on PC see also section 3.6). Notably, an additional peak, at a lower energy (1 meV), is clearly visible in the dynamic structure factor of the sample where only rapidly exchanging protons have been substituted by deuterium.

Phenomenologically, a single Lorentzian, centred at about 3.5 meV reproduces the dynamic structure factor of the sample where both rapidly and slowing exchanging protons have been substituted by deuterium [59]. Two Lorentzians, one centred at about 1 meV and another one centred at about 3.5 meV, are required to fit the dynamic structure factor of the sample where only rapidly exchanging protons have been replaced by deuterium (see figure 8 and its legend) [59]. Notably, the same parameters describing the Lorentzian centred at 3.5 meV can be used for both samples.

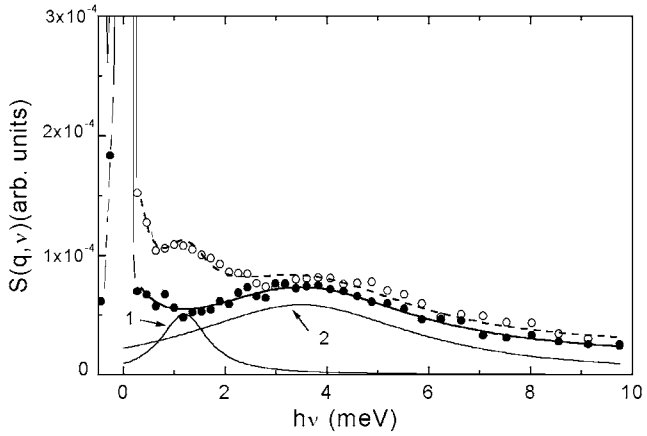

Figure 8. Experimental dynamic structure factor, $S(q, \nu)$, as function of $h\nu$, at $q = 1.5$ Å^{-1}, at 100 K, of D_2O hydrated PC (0.40 g of D_2O/g of protein). Full circles: rapidly and slowly exchanging protein protons have been substituted by deuterium; open circles: rapidly exchanging protein protons have been substituted by deuterium. Curve 1: Lorentzian lineshape $\frac{A_1}{[(E-E_1)^2+\sigma_1^2]}$, with parameters $A_1 = 3.9^{-5}$, $E_1 = 1.0$ meV, $\sigma_1 = 0.9$ meV; curve 2: Lorentzian lineshape $\frac{A_2}{[(E-E_2)^2+\sigma_2^2]}$, with parameters $A_2 = 4.4 \times 10^{-4}$. $E_2 = 3.5$ meV, $\sigma_2 = 2.7$ meV. Dashed curve: superposition of curves 1, 2 and a ground. Dotted curve: superposition of curve 2 and a ground. Adapted from [59].

Generally, these results point out that exchangeable and non-exchangeable protein protons reveal different vibrational features. In particular, the boson peak, at 3.5 meV is essentially due to non-exchangeable protein protons, while the peak at 1 meV is to be attributed to the slowly exchangeable ones. Since the slowly exchangeable protein protons, located in the amide groups of the backbone, are involved in the intramolecular H-bond network stabilizing the macromolecule structure, the peak at 1 meV might be related to the fluctuations of the H-bonds.

The appearance of a vibrational state excess in the INS spectra is a feature observed in many glassy systems [98, 125, 126], and it has been generally attributed to topological disorder [127]. It might originate from structural correlations over an intermediate range scale, associated with localized excitations; vibrations at and below such a peak coexisting and interacting with sound waves [125, 127–130]. The evidence that an excess of vibrational modes has been observed in INS spectra of both heat and acid denatured myoglobin [42] and a mixture of hydrated amino acids [92] indicating that the vibrations corresponding to the peak are independent of the main-chain conformation and packing and of the monomer chemical linkage [42].

3.5. MD simulation of inelastic incoherent neutron scattering

The MD dynamic structure factor, $S(\mathbf{q}, \nu)$, of D_2O hydrated AZ, calculated as function of energy for all the hydrogen atoms, is shown in figure 9 for four different temperatures (100, 180, 220 and 300 K) at $q = 1.8$ Å^{-1}. It can be seen that a low-frequency inelastic band centred around approximately 1.5 meV is clearly visible at low temperatures up to 220 K. The presence of the boson peak can also be put into evidence in the density of the states (see the inset of figure 9) where the ratio $g(\nu)/\nu^2$ shows for various temperatures a bump of low-frequency modes located at about 1.5 meV. Such a peak has been detected at higher energies if the Ewald

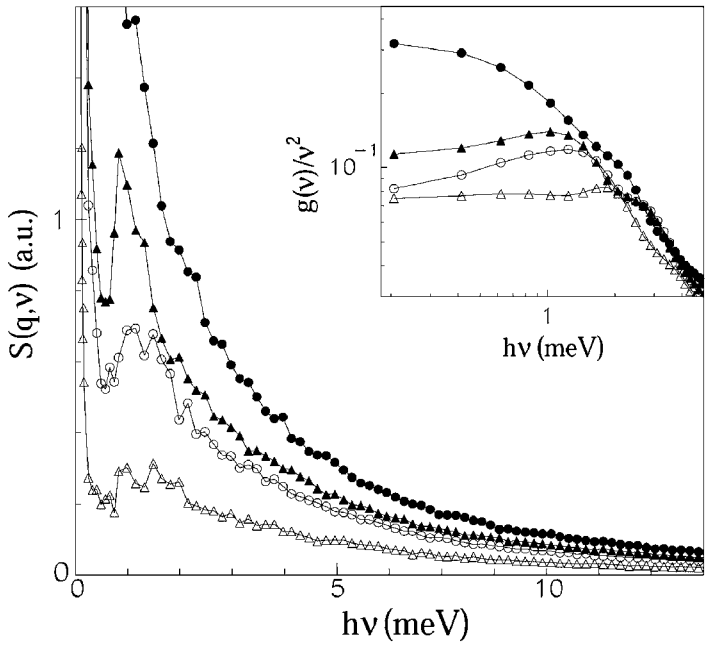

Figure 9. MD simulated dynamic structure factor, $S(q, \nu)$, as a function of $h\nu$, at $q = 1.8$ Å^{-1}, of D_2O hydrated AZ (0.36 g of D_2O/g of protein) at different temperatures: 100 K (open triangles), 180 K (open circles), 220 K (full triangles) and 300 K (full circles). Inset: MD calculated vibrational density of states divided by ν^2 as a function of energy. Adapted from [43].

sums to treat the long-range interactions are introduced [131] or, alternatively, if a few proteins are inserted in a monoclinic cell [132]. This suggests that the 1.5 meV peak, observed when MD simulations in the single molecule configuration are performed, could be mainly due to short range interactions [28, 45, 95].

With the aim of investigating by MD the contribution to the inelastic bump of various protein atoms, the AZ hydrogen atoms have been divided into five classes according to their mobility as evaluated by the mean square fluctuation values. Then, the contribution to the dynamic structure factor from hydrogens in each class has been determined. The results are shown in figure 10 for 300 K and in the related inset for 100 K. At 100 K, the inelastic bump, peaking at about 1.5 meV, appears evident for each class of the hydrogens, and it becomes more and more well-shaped as long as smaller mean square fluctuations are taken into account. Therefore, hydrogens characterized by low mobility give the most significant contribution to the boson peak.

At 300 K, the quasielastic part of the spectrum overlaps quite extensively with the inelastic peak and only when low mean square fluctuation values are considered can the peak be clearly detected in the spectra. In addition, even if the quasielastic interference with the inelastic contribution does not allow us to extract the inelastic part at 300 K, the persistence of such an excess of vibrational modes can be clearly observed also at this temperature. Such a result is particularly interesting in connection with some theoretical findings which discriminate between systems in which the boson peak is or is not present at high temperature [114, 133]. The persistence of the inelastic peak at high temperature might be interpreted as an indication of a 'strong' amorphous character according to the nomenclature in [134].

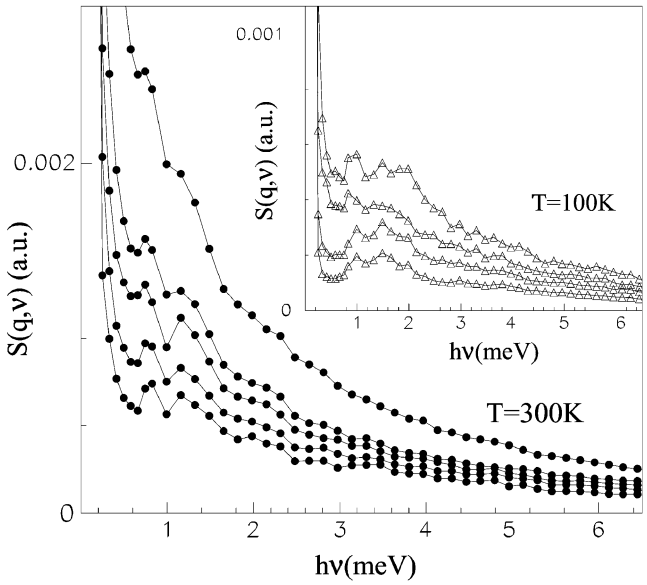

Figure 10. MD simulated dynamic structure factor, $S(q, \nu)$, as a function of $h\nu$, at $q = 1.8$ Å^{-1}, for hydrogens with different mean square fluctuation values of D_2O hydrated AZ (0.40 g of D_2O/g of protein) at 300 K. From the bottom to the top, mean square displacement ranges (in Å^2): [0.1–0.2], [0.2–0.3], [0.3–0.4], [0.4–0.5] and [0.5–∞]. Inset: same as in main figure but at $T = 100$ K and with the following mean square fluctuation ranges from the bottom to the top (in Å^2): [0–0.1], [0.1–0.2], [0.2–0.3] and [0.3–∞]. Each spectrum has been normalized to the number of atoms belonging to the corresponding class. Adapted from [53].

3.6. Inelastic incoherent neutron scattering and MD simulation of hydration water

The dynamical properties of the solvent surrounding the ET protein can be highlighted by comparing the INS spectra of a protein hydrated by D_2O or H_2O. Figure 11(a) shows the experimental dynamic structure factor, $S^{PC+D_2O}(2\theta, \nu)$ of D_2O hydrated PC. Generally, the observed spectral features of PC appear to be quite similar to those of AZ. By restricting our analysis to the inelastic region, we note the presence of a broad peak, centred at about 3.5 meV, clearly visible at 100 and 220 K and possibly merging into the broad quasielastic contribution at 300 K. The dynamic structure factor, $S^{PC+H_2O}(2\theta, \nu)$, of H_2O hydrated PC is shown in figure 11(b) for the same three temperatures and scattering angle of those of figure 11(a). Again, the low temperature curves reveal, in the inelastic region, a peak located at approximately 3.5 meV, over which the quasielastic contribution superimposes at 300 K. Now, both the protein and the hydration water protons contribute to the dynamic structure factor. With the aim of extracting the contribution of the water solvent to the total dynamic structure factor, both $S^{PC+D_2O}(2\theta, \nu)$ and $S^{PC+H_2O}(2\theta, \nu)$ have been carefully normalized by taking into account the number of the protein protons in the samples [56, 62] (see also legend of figure 11). Accordingly, the difference:

$$S^{H_2O}(2\theta, \nu) = S^{PC+H_2O}(2\theta, \nu) - S^{PC+D_2O}(2\theta, \nu) \tag{19}$$

provides information about the dynamics of the water molecules belonging to the hydration shell around PC. The extracted dynamic structure factor, $S^{H_2O}(2\theta, \nu)$, is shown in figure 11(c). A broad peak, centred at about 3.5 meV, is well visible at 100 and 220 K, whereas it likely appears to be masked by the quasielastic contribution at 300 K. However, it should be taken into account that $S^{H_2O}(2\theta, \nu)$ contains a contribution from both the hydration shell and the

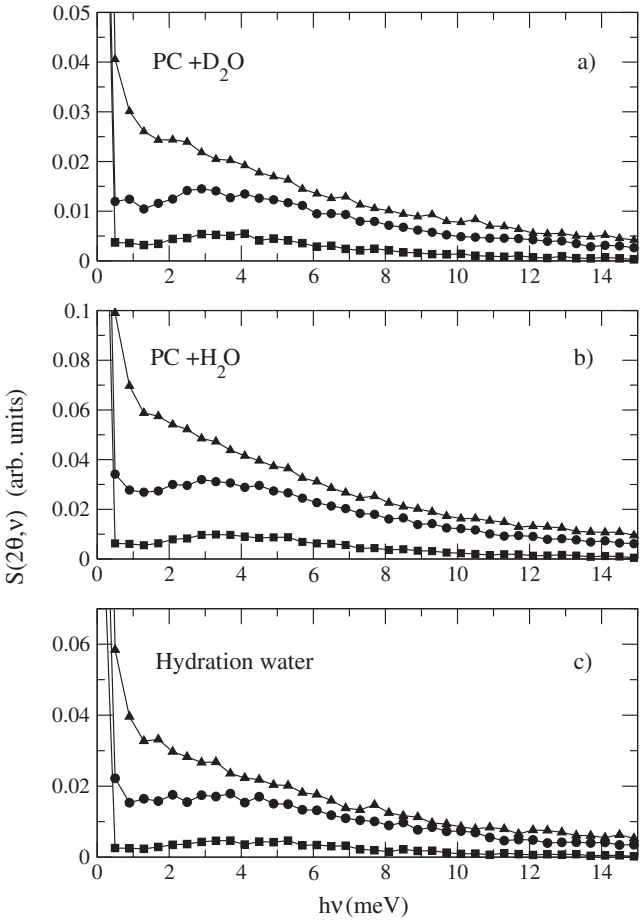

Figure 11. Experimental dynamic structure factor, $S(2\theta, \nu)$, as a function of $h\nu$, at $2\theta = 88°$, of (a) D_2O hydrated PC (0.38 g of D_2O/g of protein), (b) H_2O hydrated PC (0.38 g of H_2O/g of protein), (c) PC hydration water for the following temperatures: 100 K (square); 220 K (circle); 300 K (triangle). Solid curves are a guide to the eye. A H_2O hydrated PC macromolecule contains 558 non-exchangeable protein protons, about 48 solvent-exposed, fast exchanging protein protons, about 100 buried protein protons with a long exchanging time and 455 H_2O solvent protons. A D_2O hydrated PC macromolecule contains 558 non-exchangeable protein protons and 50 protein protons with a long exchanging time (under the assumption that about 50% of slow exchangeable protons have actually exchanged with deuterium solvent, according to [62]). Data have been normalized to the energy integral $\int S(2\theta, \nu)h\,\mathrm{d}\nu$ in the whole energy range. Adapted from [58].

exchangeable PC protons; the latter being about 14% of the total. On the other hand, the inelastic peak is about five times higher than that expected if only exchangeable protein protons would have contributed [58]. Such a finding strongly supports the existence of an excess of low frequency vibrational modes in the hydration shell surrounding PC. Notably, such an excess practically appears at the same energy at which it has been observed in the protein; while such a peak has been not observed in the neutron scattering of hydrated phycocyanin (fully deuterated) [66] and hydrated myoglobin [62]. Moreover, a similar vibrational anomaly has been detected in supercooled water confined in pores of Vycor glass [135].

Figure 12 shows the MD simulated dynamic structure factor, $S_{\mathrm{inc}}(q, \nu)$, of protein hydration water [55]. It turns out that at temperatures up to 180 K, a broad inelastic bump

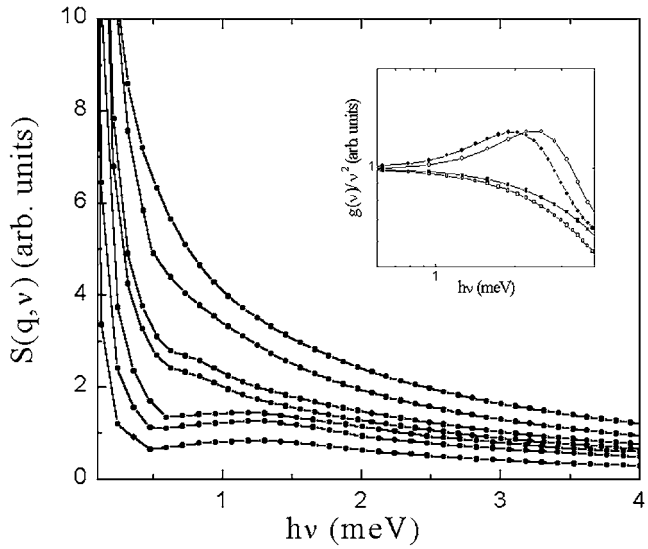

Figure 12. MD simulated dynamic structure factor, $S(q, \nu)$, as a function of $h\nu$, at $q = 2$ Å^{-1}, of protein hydration water. The temperatures are 100, 150, 180, 200, 220, 260 and 300 K from bottom to top. Inset: density of states divided by ν^2 as a function of energy at 100 K (open circles), 180 K (full circles), 200 (full squares), 220 K (open squares). Solid curves are a guide to the eye. Adapted from [55].

appears well visible in the low-frequency region, peaking at about 1.5 meV similar to what observed in [47]. By increasing the temperature this peak becomes less and less distinct due to the rising intensity of the quasielastic contribution. The density of states, $g(\nu)$, of hydration water, computed as Fourier transform of the velocity autocorrelation function $C_{vv}(t)$ (see equation (16)), shown in the inset of figure 12 reveals an excess of vibrational modes at about 1.5 meV for temperatures below 180 K. At higher temperatures (220 and 300 K), a Debye-like behaviour is registered in the low-frequency region (see inset of figure 12). It is worth noting that the boson peak of protein hydration water, as detected by MD simulation, is again located at the same energy at which it is observed in the protein; the same behaviour having also been observed in the hydration water of AZ [57]. Furthermore, the existence of the boson peak has also been revealed in the hydration water of ribonuclease A [132, 47]; such a bump being detected at a higher energy when MD simulation is carried out in the presence of a cluster of protein molecules. Remarkably, the existence of the boson peak in the PC hydration water was first predicted by MD simulation [55] and subsequently confirmed by neutron scattering measurements [56].

The simultaneous presence of a boson peak in the protein and in the hydration water provides further support for an extensive dynamical coupling between the protein and the surrounding solvent. For the ET proteins, we suggest that the presence of the boson peak in the hydration water could reflect the crucial role of water into the regulation of the ET process.

3.7. Quasielastic incoherent neutron scattering

The dynamic structure factor of D_2O hydrated AZ shows a significant broadening of the elastic peak by increasing the temperature (see figure 3); such a broadening arising from protein diffusion and relaxational movements. Due to the high complexity of the protein structure, many different kinds of motions may contribute to the quasielastic scattering: motions of

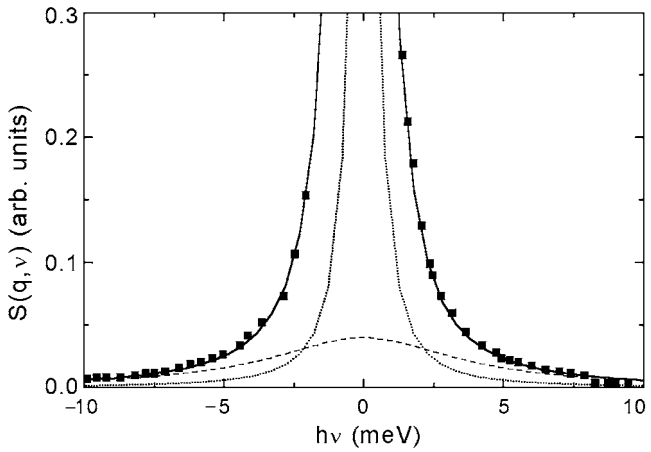

Figure 13. Experimental neutron scattering data of D_2O hydrated AZ (0.40 g of D_2O/g of protein) at 300 K. Full curve: best fit function. Dashed curve: slow Lorentzian component ($\sigma = 34$ μeV). Dotted curve: fast Lorentzian component ($\sigma = 3.3$ μeV).

the methyl groups and of protons in hydrogen bonds, reorientations of side-chains, etc [36]. These motions can generally be modelled in terms of jump diffusions involving two or three states [36]. Phenomenologically, the quasielastic broadening in proteins can be described with a sum of Lorentzians; each Lorentzian representing a continuous distribution of motions with a different amplitude. In our case, two Lorentzian curves (see curves in figure 13) are practically sufficient to reproduce the quasielastic broadening of D_2O hydrated AZ at 300 K; a similar behaviour having been observed for other protein systems [8, 35].

The quasielastic contribution to the scattering, $S_{\mathrm{qel}}(q, \nu)$, has been extracted from the total incoherent neutron scattering and shown in the log–log plot in figure 14(a) for the D_2O hydrated and dry AZ at 300 K. From this figure, it is apparent that both the samples approximately exhibit the same trend. However, the corresponding intensities differ by a scale factor; the dry sample being characterized by a lower intensity.

The quasielastic contribution of AZ has been analysed by a model function containing two power law components [29, 92] which takes into account slow and fast dynamical processes, respectively:

$$S_{\mathrm{qel}}(q, \nu) \propto A\nu^{-1-b} + B\nu^{-1+a}. \tag{20}$$

Notably, equation (20) becomes equivalent to a sum of two Lorentzians for $a = -1$ and $b = 1$. Furthermore, for a Brownian motion of large particles suspended in a solvent composed of many small particles, the quasielastic spectra exhibit one component corresponding to diffusion of large particles ($b = 1$ and $a = 1$) and another one (white noise), describing the much faster dynamics of the solvent ($b = -1$ and $a = 1$).

A fit of the quasielastic spectra with equation (20) of D_2O hydrated and dry AZ is shown in figure 14(a) for the two samples. Even though the calculated values a and b are quite scattered ($a = 0.45 \pm 0.15, b = 0.5 \pm 0.15$ for hydrated AZ and $a = 0.40 \pm 0.15, b = 0.55 \pm 0.15$ for dry AZ), it can be observed that the curves corresponding to the two power laws intersect at nearly the same energy (approximately 0.4 meV) in both samples, indicating that the characteristic times involved in the diffusive processes are independent of the hydration level. In addition, these values are comparable with those derived for myoglobin [42] suggesting that globular proteins have quite similar characteristic relaxational times, irrespective of both their secondary and tertiary structure.

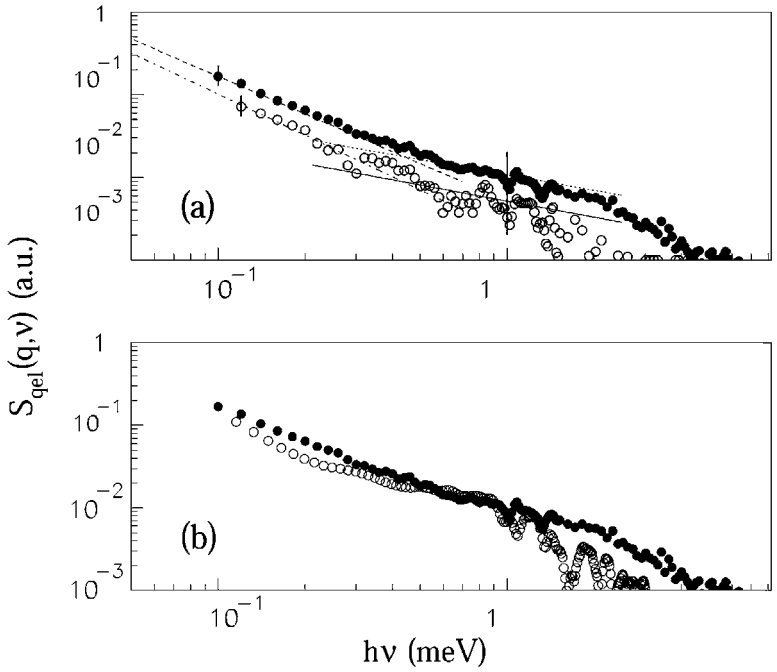

Figure 14. (a) Experimental quasielastic neutron scattering intensity, as a function of $h\nu$, at $q = 1.8$ Å^{-1} of D_2O hydrated (0.36 g of D_2O/g of protein) (full symbols) and dry (open symbols) AZ sample at $T = 300$ K together with the result of the fit with the two-power law equation (20). The data have been extracted from the total scattering spectrum by applying equations (10) and (11) with $T_0 = 100$ K. (b) Experimental (full symbols) and MD simulated (open symbols) quasielastic neutron scattering intensity, as a function of $h\nu$, at $q = 1.8$ Å^{-1}, of D_2O hydrated AZ sample at $T = 300$ K. Adapted from [43].

The observed results for (a) and (b) find a correspondence in the framework of the mode coupling theory (MCT) which accounts for the dynamics of glasses in terms of a damped oscillator with memory [114, 108]. According to this theory, the observed quasielastic scattering of AZ can be interpreted as a superposition of fast, β, local motions of particles in the cage formed by neighbours and slow, α, collective motions arising from the rearrangement of the cages, in agreement with the results on myoglobin [42, 29]. Alternatively, the protein motion probed by quasielastic neutron scattering has been described in terms of diffusion in spheres with a distribution of radii; the average sphere radius for the backbone atoms turning out to be significantly smaller than for the side chains [136]. The evidence of a non-exponential relaxation for diffusive motions of both backbone and side chain atoms suggests a close relationship of such a radially softing diffusive approach with that based on MCT. Furthermore, the progressively more difficult reorganization as procession from the side chains to the backbone atoms for the internal protein motions occurs well mimics the collective and the local motions described by α and β relaxations in the MCT [108].

All these results, further supporting the amorphous character of protein systems, provide a unifying vision of protein dynamics in which fast, local motions could trigger large amplitude, functionally relevant, motions.

In figure 14(b), together with the experimental data, the MD computed quasielastic contributions at room temperature are shown (see section 2). The simulated scattering agrees quite well with the experimental one, especially between 0.4 and 1 meV, while at low energies

the two curves display different trends. Since the low-energy range spectra are determined by the slow collective motions, the observed discrepancy could again be ascribed to the fact that the long-range interactions have been neglected in our single molecule MD simulation.

To discriminate between the quasielastic and inelastic scattering, the contribution to the quasielastic and inelastic part of the spectrum has been estimated, from MD simulation data, for each hydrogen atom i (for details see [53]). It turns out that the inelastic scattering is prevalent at 100 K, while diffusion is dominant at 300 K. In addition, hydrogens belonging to the β-sheets as well as to the α-helix region are mainly characterized by an inelastic character, while hydrogen atoms located in turns reveal a prevailing diffusive behaviour. Finally, it has been found that the regions involved into the binding interaction to the ET partners exhibit a diffusive character consistent with an expected higher flexibility for these regions [53].

Therefore, a simultaneous analysis of both the inelastic and quasielastic properties of a protein could provide some information relevant to understanding how the functional role is connected with the structural and dynamical properties of the system.

3.8. Protein dynamics and the electron transfer process

The intermolecular ET process in biological systems involves several reaction steps, such as binding of proteins, structural rearrangements, chemical transformations etc [1]. In addition, since the redox centres of the electron donor and acceptor proteins are separated by long distances, the protein milieu takes an active part in the ET reaction. First, it should provide the structural support to the active site whose architecture is to be preserved to correctly perform the functional role. Additionally, it must guarantee some flexibility to the redox centre in order to allow a fine tuning of the ET properties. At the same time, protein flexibility is also required to appropriately perform the binding to the physiological partners. Finally, the protein provides the medium where the electron tunnelling takes place. The surrounding solvent, besides stabilizing the protein structure can be also involved into the ET process of the redox chain [1, 137]. Thermal fluctuations of the solvent, through a modulation of the protein dynamics, can mediate the electron path from the donor to the acceptor.

Briefly, in the framework of the Marcus classical theory, the non-adiabatic ET rate can be expressed in the form [1, 138]:

$$k_{\mathrm{ET}} = \frac{4\pi^2 H_{\mathrm{AB}}^2}{h\sqrt{(4\pi^2 \lambda RT)}} \exp\left(-\frac{(\Delta G^{\mathrm{o}} + \lambda)^2}{4\lambda k_{\mathrm{b}} T}\right) \tag{21}$$

where H_{AB} is the electronic coupling matrix between the donor and the acceptor, ΔG^{o} is the driving force determined by the redox potential differences for the reaction, and λ is the reorganization energy which takes into account the energy required to distort the equilibrium nuclear geometry of the reactant state into that of the product state without ET [1]. The reorganization energy λ can be separated into a contribution from the vibrations of the protein and another one from the solvent [1].

Although the results concerning AZ and PC and their solvent do not directly relate to the ET process, they can provide some insight into the dynamical aspects strictly involved in the ET reaction. Indeed, both the general and the specific dynamical properties of AZ and PC may result in a modulation of the k_{ET} ET rate.

The glassy character of ET proteins can be interpreted in terms of the so-called multipath approach [139]. It has been hypothesized that the electron can pass from the donor to the acceptor through a variety of paths [139]. Actually, electron tunnelling might occur via a family of non-equivalent pathways to which covalent bonds, hydrogen bonds and through-space jumps can contribute [3]; such a multiplicity can be relevant for the ET rate, through a modulation of the electronic coupling matrix values [139]. In more detail, two approaches can

be taken into account. First, a single molecule can offer, to the electron, multiple paths. Second, each molecule provides the same electronic path which, on the other hand, may produce slightly different results from molecule to molecule due to the structural heterogeneity in the protein ensemble. Therefore, in both cases, the topological disorder, determining a heterogeneity in the biological answer, may significantly affect the ET process in the AZ and PC protein systems.

The amorphous character of hydration water of AZ and PC can further contribute to the ET process from different points of view. On the one hand, since their is strong dynamical coupling between the protein and the hydration water, the solvent, by injecting its dynamics on the macromolecule, can amplify the multiplicity of the ET paths in the protein. On the other hand, the hydration water itself, by directly taking part in the ET rate, may give a contribution to the multipathways regime. The latter aspect is also supported by the Onuchic–Wolynes model [137, 140] for which the polarization properties of the solvent might give rise to equivalent diffusion paths controlling the ET reaction.

The presence of the boson peak, besides providing further evidence for the amorphous character of the analysed protein systems, may offer additional elements to the interplay between the dynamical properties and the ET process in AZ and PC. The boson peak, related to a strong scattering of acoustic phonons, has been hypothesized to originate from structural correlations over an intermediate range scale. Indeed, collective vibrational modes form part of the reaction coordinates of the functional motions of proteins [121]. Accordingly, the excess of vibrational modes might be in some way involved into the coherent movements required to perform the ET transfer reaction steps [43]. Such a picture is also supported by the simultaneous presence of the boson peak, at the same energy, in both the protein and the hydration water; such a coincidence, likely a peculiarity of ET proteins, pointing toward some implications of this vibrational anomaly on their functionality.

Finally, it should be remarked that a detailed knowledge of the dynamics of ET proteins, ranging from high frequency well-defined localized modes to very low frequency delocalized modes, is required to reach a full understanding of the ET process. Neutron scattering in connection with MD simulations offer the possibility to deeply investigate fast motions of protein dynamics. We mention that these motions might be crucial in determining reaction rates in proteins. In this respect, a MD simulation of an AZ study has revealed that fast macromolecular fluctuations can modulate the numerical value of the electronic coupling matrix H_{AB} [5]; the tunnelling electron being capable of emitting or absorbing vibrational energy.

4. Conclusions and perspectives

A variety of motions, covering a wide temporal and spatial range, of ET proteins can be monitored by INS. An analysis of the elastic, quasielastic, inelastic spectra, as a function of temperature, providing the dynamical behaviour of the hydrogens uniformly distributed over the macromolecule, allows one to obtain information about different motions of the ET proteins.

Additionally, INS investigation of protein samples, hydrated by H_2O or D_2O makes it possible to obtain information on the dynamical behaviour of the solvent around a macromolecule. Such an aspect is particularly relevant since the dynamics of proteins has emerged as being strongly determined by that of solvent.

The capabilities of INS can be drastically amplified when used in connection with MD simulations. The contributions to the neutron scattering arising from different protein atomic classes, or from a specific region of the macromolecule, can be separately extracted from the

total scattering. In other words, a conjugated approach by INS and MD simulation offers the possibility of scaling down from global to local dynamics, still maintaining a close connection with the experimental data.

Generally, the dynamical properties of ET proteins exhibit many similarities with those of other proteins and, in particular, with that of myoglobin which, being one of the most studied proteins, represents a sort of benchmark for protein dynamics [103]. In this respect, we remark that a detailed knowledge of the dynamical behaviour for a variety of proteins, with a different functional role, could be crucial to discriminate between universal and specific features in protein dynamics. This knowledge also constitutes a necessary step to reach a full understanding of the relationship between structure, dynamics and functionality of biomolecules. These aspects are of utmost importance in our proteomic *era* to connect the structure, or even the sequence, to the functionality by contributing them to solving the protein puzzle whose final solution requires a large, coordinated effort.

The dynamics of the ET proteins AZ and PC, as emerging from INS and MD simulation data, exhibits two general aspects: a glassy, amorphous character and a strong protein–solvent dynamical coupling. Both these aspects, shared with other globular proteins, might have implications for the specific functional role of these systems.

As already mentioned, the glassy character of proteins can be related to the complexity of their energy landscape. The number of interacting atoms, the variety of the involved interactions, with short, medium and long range, can be assumed to give rise to the existence of many, nearly isoenergetic local minima, hierarchical organized, in the energy landscape. At the same time, such a complexity might be at the origin of the peculiar dynamical behaviour observed in proteins, such as the onset of anharmonic motions, the fast and slow relaxations in diffusive motions and the excess of vibrational modes.

The INS and MD simulation results clearly point out a strong protein–solvent dynamical coupling in the ET proteins. Such a result confirms the hypothesis that the protein dynamics is drastically regulated by the dynamical properties of the surrounding solvent. On the other hand, hydration water of AZ and PC exhibits an glassy character similar to what observed in other protein systems. The appearance of an excess of vibrational modes in the hydration water around the ET proteins is particularly interesting in connection to the simultaneous presence of a similar excess in these proteins. It should be speculated that the structural properties of AZ and PC could possibly determine a peculiar organization of the solvent. Accordingly, the protein and the surrounding solvent may constitute a unique object whose global properties can regulate the ET process.

Although INS has been widely employed to investigate the dynamics of different proteins, the potentialities of such a technique are still partially unexpressed. Among others, we would like to mention two possible developments: a much larger use of controlled H/D contrast and the extension of INS to study proteins adsorbed on surfaces [141]. The first aspect could offer the possibility of separately analysing the dynamical behaviour of hydrogens localized in particular regions or with some specific functional role; e.g. hydrogens belonging to regions involved into the ET process or into the binding to the ET protein partners.

On the other hand, the investigation by INS of biomolecules adsorbed onto surfaces is particularly relevant for ET proteins. Recently, ET proteins, and in particular AZ and PC, covalently bound to metallic substrates, have gained considerable interest for their ET capability which can be exploited for applications in molecular biosensors and nanodevices [2, 142–144]. The study and the optimization of the heterogeneous (biomolecule-conductive electrodes) ET mechanism requires a full characterization of the dynamics of the protein anchored to a surface; changes in protein dynamics, likely related to the new spatial organization, could be clarified by neutron scattering. However, such an approach considering samples with a small amount

of matter requires a large neutron flux; this could be soon feasible with the development of a new generation of neutron sources.

Acknowledgments

I would like to thank Salvatore Cannistraro for his continuous support and his critical reading of the manuscript.

References

[1] Marcus R A and Sutin N 1985 *Biochem. Biophys. Acta* **265** 265
[2] Shifman J M, Gibney B R, Sharp R E and Dutton P L 2000 *Biochemistry* **39** 14813
[3] Beratan D N, Betts J N and Onuchic J N 1991 *Science* **252** 1285
[4] Hammes-Schiffer S 2002 *Biochemistry* **41** 13335
[5] Daizadeh I, Medvedev E S and Stuchebrukhov A A 1997 *Proc. Natl Acad. Sci. USA* **94** 3703
[6] Arcangeli C, Bizzarri A R and Cannistraro S 2001 *Biophys. Chem.* **90** 45
[7] Gregory R B 1995 *Protein–Solvent Interactions* (New York: Dekker)
[8] Bizzarri A R and Cannistraro S 2002 *J. Phys. Chem.* B **106** 6617
[9] Teeter M M 1991 *Annu. Rev. Biophys. Biophys. Chem.* **20** 577
[10] Kuntz I D and Kauzmann W 1974 *Adv. Protein Chem.* **28** 239
[11] Rupley J L and Careri G 1991 *Adv. Protein Chem.* **41** 37
[12] Poole P L and Finney J L 1983 *Biopolymers* **22** 255
[13] Denisov V P and Halle B 1996 *Faraday Discuss.* **103** 227
[14] Doniach S 2001 *Chem. Rev.* **101** 1763
[15] Parak F, Knapp E W and Kucheida D 1982 *J. Mol. Biol.* **161** 177
[16] Goldanskii V I and Krupyanskii Y F 1989 *Q. Rev. Biophys.* **22** 39
[17] Cantor C R and Schimmel P R 1980 *Biophysical Chemistry* part II*: Techniques for the Study of Biological Structure and Thermodynamics* (New York: Wiley)
[18] Spiro T G and Czernuszewicz R 1985 *Methods Enzymol.* **246** 416
[19] Petry R, Schhmitt M and Popp J 2003 *Chem. Phys. Chem.* **4** 14
[20] Clore G M and Schwieters C D 2002 *Curr. Opin. Struct. Biol.* **12** 146
[21] Cannistraro S, Bizzarri A R and Guzzi R 1997 *Trends Chem. Phys.* **5** 25
[22] Lovesey S 1986 *Theory of Neutron Scattering from Condensed Matter* (Oxford: Oxford Science)
[23] Gabel J, Lehenert U, Tehei M, Weik M and Zaccai G 2002 *Q. Rev. Biophys.* **35** 327
[24] Middendorf H D 1996 *Physica* B **226** 113
[25] Reat V, Patzelt H, Pfister C, Ferrand M, Oesterhelt D and Zaccai G 1998 *Proc. Natl Acad. Sci. USA* **95** 4970
[26] Perez J, Zanotti J M and Durand D 1999 *Biophys. J.* **77** 454
[27] Bee M 1988 *Quasielastic Neutron Scattering: Principles and Applications in Solid-State Chemistry Biology and Material Science* (Bristol: Hilger)
[28] Smith J C 1991 *Q. Rev. Biophys.* **24** 227
[29] Doster W, Cusack S and Petry W 1989 *Nature* **337** 754
[30] Ferrand M, Dianoux A J, Petry W and Zaccai G 1993 *Proc. Natl Acad. Sci. USA* **90** 9668
[31] Andreani C, Filabozzi A, Menzinger F, Desideri A, Deriu A and Di Cola D 1995 *Biophys. J.* **68** 2519
[32] Daniel R M, Smith J C, Ferrand M, Hery S, Dunn R and Finney J L 1998 *Biophys. J.* **75** 2504
[33] Zaccai G 2000 *Biophys. Chem.* **86** 249
[34] Zaccai G 2000 *Science* **288** 1604
[35] Fitter J, Lechner R E and Dencher N A 1997 *Biophys. J.* **73** 2126
[36] Fitter J, Lechner R E, Bueldt G and Dencher N A 1996 *Proc. Natl Acad. Sci. USA* **93** 7600
[37] Middendorf H D 1994 *Q. Rev. Biophys.* **13** 425
[38] Bellissent-Funel M C, Zanotti J M and Chen S H 1996 *Faraday Discuss.* **281** 281
[39] Perez J, Zanotti J M and Durand D 1999 *Biophys. J.* **77** 454
[40] Doster W, Cusack S and Petry W 1990 *Phys. Rev. Lett.* **65** 1080
[41] Giordano R, Salvato G, Wanderkingh F and Wanderlingh U 1990 *Phys. Rev.* A **41** 689
[42] Cusack S and Doster W 1990 *Biophys. J.* **58** 243
[43] Paciaroni A, Stroppolo M E, Arcangeli C, Bizzarri A R, Desideri A and Cannistraro S 1999 *Eur. Biophys. J.* **28** 447

[44] Kneller G R, Keiner V, Kneller M and Schiller M 1995 *Comput. Phys. Commun.* **91** 191
[45] Steinbach P J, Loncharich R J and Brooks B R 1991 *Chem. Phys.* **158** 383
[46] Cusack S, Smith J, Finney J, Tidor B and Karplus M 1988 *J. Mol. Biol.* **202** 903
[47] Tarek M and Tobias D J 2000 *Biophys. J.* **79** 3244
[48] Kneller G R, Doster W, Settles M, Cusack S and Smith J C 1992 *J. Chem. Phys.* **97** 8864
[49] Smith J C, Kuczera K and Karplus M 1990 *Proc. Natl Acad. Sci. USA* **87** 1601
[50] Chen S H, Gallo P, Sciortino F and Tartaglia P 1997 *Phys. Rev.* E **56** 4231
[51] McCammon J A and Harvey S C 1987 *Dynamics of Protein and Nucleic Acids* (Cambridge: Cambridge University Press)
[52] Brooks C L III, Karplus M and Pettitt B M 1988 *Proteins: a Theoretical Perspective of Dynamics Structure and Thermodynamics* (New York: Wiley–Interscience)
[53] Paciaroni A, Bizzarri A R and Cannistraro S 2000 *J. Mol. Liq.* **84** 3
[54] Adman E T 1985 *Structure and Function of Small Blue Copper Proteins* part I (*Topics in Molecular and Structural Biology: Metalloproteins* vol 6) ed P M Harrison (Weinheim: Chemie Verlag)
[55] Paciaroni A, Bizzarri A R and Cannistraro S 1998 *Phys. Rev.* E **57** 6277
[56] Paciaroni A, Bizzarri A R and Cannistraro S 1999 *Phys. Rev.* E **60** 2476
[57] Paciaroni A, Bizzarri A R and Cannistraro S 1999 *Physica* B **269** 409
[58] Bizzarri A R, Paciaroni A and Cannistraro S 2000 *Phys. Rev.* E **62** 3991
[59] Bizzarri A R, Paciaroni A, Arcangeli C and Cannistraro S 2001 *Eur. Biophys. J.* **30** 443
[60] Frauenfelder H, Petsko G A and Tsernoglou D 1979 *Nature* **280** 558
[61] Reat V, Dunn R, Ferrand M, Finney J L, Daniel R M and Smith J C 2000 *Proc. Natl Acad. Sci. USA* **97** 9961
[62] Settles M and Doster W 1996 *Faraday Discuss. R. Soc. Chem.* **103** 269
[63] Orecchini A, Paciaroni A, Bizzarri A R and Cannistraro S 2001 *J. Phys. Chem.* B **106** 6617
[64] Orecchini A, Paciaroni A, Bizzarri A R and Cannistraro S 2002 *J. Phys. Chem.* B **106** 7348
[65] Schoenborn B P, Ramakrishnan V and Schneider D 1986 *Physica* B +C **137** 214
[66] Bellissent-Funel M C, Teixeira J, Bradley K F, Chen S H and Crespi H L 1992 *Physica* B **181** 740
[67] van Gunsteren W F and Berendsen H J C 1991 *Angew. Chem. Int. Edn Engl.* **29** 992
[68] MacKerrell A D Jr, Bashford D, Bellott M, Dunbrack R L Jr, Evanseck J D, Field M J, Fischer S, Gao J, Guo H, Ha S, Joseph-McCarthy D, Kuchnir L, Kuczera K, Lau F T K, Mattos C, Michnick S, Ngo T, Nguyen D T, Prodhom B, Reiher W E III, Roux B, Schlenkrich M, Smith J C, Stote R, Straub J M, Watanabe M, Wiorkiewicz-Kuczera J, Yin D and Karplus M 1998 *J. Phys. Chem.* B **102** 3586
[69] van Gunsteren W F and Berendsen H J C 1987 *Groningen Molecular Simulation (GROMOS) Library Manual* (Groningen: Biomos)
[70] Cornell W D, Cieplak P, Bayly C I, Gould I R, Merz K M Jr, Ferguson D M, Spellmeyer D C, Fox T, Caldwell J W and Kollman P A 1995 *J. Am. Chem. Soc.* **117** 5179
[71] Levitt M, Hirshberg M, Sharon R and Daggett V 1995 *Comput. Phys. Commun.* **91** 215
[72] Berendsen H J C, Postma J P M, van Gunsteren W F and Hermans J 1981 *Intramolecular Forces* ed B Pulman (Dordrecht: Reidel) p 33
[73] Berendsen H J C, Grigera J R and Straatsma T P 1987 *J. Phys. Chem.* **91** 6269
[74] Jorgensen W L, Chandrasekhar J, Madura J D, Impey R W and Klein M L 1983 *J. Chem. Phys.* **79** 926
[75] Levitt M, Hirshberg M, Sharon R, Laidig K E and Daggett V 1997 *J. Phys. Chem.* B **101** 5051
[76] Stillinger F H and Rahman A 1974 *J. Chem. Phys.* **60** 1545
[77] Allen M P and Tildesley D J 1987 *Computer Simulation of Molecular Liquids* (Oxford: Clarendon)
[78] Steinbach P J and Brooks B R 1994 *J. Comput. Chem.* **15** 57
[79] Barker L A and Watts R O 1973 *Mol. Phys.* **26** 789
[80] Darden T, York D and Pedersen L 1993 *J. Chem. Phys.* **98** 10089
[81] Smith P E, Blatt H D and Pettitt B M 1997 *J. Phys. Chem.* B **101** 3886
[82] Ryckaert J P, Ciccotti G and Berendsen H J C 1977 *J. Comput. Phys.* **23** 327
[83] Seno Y and Go N 1990 *J. Mol. Biol.* **216** 111
[84] Farver O, Blatt Y and Pecht I 1982 *Biochemistry* **21** 3553
[85] Redinbo M R, Yeates T O and Merchant S 1994 *J. Bioener. Biomembr.* **26** 49
[86] Guss J M, Bartunik H D and Freeman H C 1992 *Acta Crystallogr.* B **48** 790
[87] Nar H, Messerschmidt A, Huber R, van de Kamp M and Canters G W 1991 *J. Mol. Biol.* **218** 427
[88] van de Kamp M, Silvestrini M C, Brunori M, Beeumen J V, Hali F G and Canters G W 1990 *Eur. J. Biochem.* **194** 109
[89] Gray H B 1986 *Chem. Soc. Rev.* **15** 17
[90] Bizzarri A R and Cannistraro S 2001 *Chem. Phys. Lett.* **349** 497
[91] Ungar L W, Scherer N F and Voth G A 1997 *Biophys. J.* **72** 5

[92] Diehl M, Doster W, Petry W and Schober H 1997 *Biophys. J.* **73** 2726
[93] Paciaroni A, Sacchetti F and Cannistraro S 2000 *Chem. Phys.* **261** 39
[94] Cannistraro S, private communication
[95] Longarich R J and Brooks B R 1990 *J. Mol. Biol.* **215** 439
[96] Nienhaus G U, Heinzl J, Huenges E and Parak F 1991 *Nature* **338** 665
[97] Fitter J 1999 *Biophys. J.* **76** 1034
[98] Frick B and Richter D 1995 *Science* **267** 1939
[99] Frauenfelder H, Parak F and Young R D 1988 *Annu. Rev. Biophys. Biophys. Chem.* **17** 451
[100] Iben I E T, Braunstein D, Doster W, Frauenfelder H, Hong M K, Johnson J B, Luck S, Ormos P, Schulte A, Steinbach P J, Xie A H and Young R D 1989 *Phys. Rev. Lett.* **62** 1916
[101] Daniel R M, Finney J L and Smith J C 2003 *Faraday Discuss.* **122** 163
[102] Doster W, Bachleitner A, Dunau R, Hiebl M and Luesher E 1986 *Biophys. J.* **50** 213
[103] Frauenfelder H, McMahon B H and Fenimore P W 2003 *Proc. Natl Acad. Sci. USA* **100** 8615
[104] Cordone L, Ferrand M, Vitrano E and Zaccai G 1999 *Biophys. J.* **76** 1043
[105] Rassmussen B F, Stock A M, Ringe D and Petsko G A 1992 *Nature* **357** 423
[106] Lee A L and Wand A J 2001 *Nature* **411** 501
[107] Bizzarri A R and Cannistraro S 2004 in preparation
[108] Goetze W and Sjoegren L 1992 *Rep. Prog. Phys.* **55** 241
[109] Ostermann A, Waschipky R, Parak F G and Nienhaus G U 2000 *Nature* **404** 205
[110] Arcangeli C, Bizzarri A R and Cannistraro S 1998 *Chem. Phys. Lett.* **291** 7
[111] Vitkup D, Ringe D, Petsko G A and Karplus M 2000 *Nat. Struct. Biol.* **7** 34
[112] Tournier A L, Xu J and Smith J C 2003 *Biophys. J.* **85** 1871
[113] Wong C F, Zheng C and McCammon J A 1989 *Chem. Phys. Lett.* **154** 151
[114] Green J L, Fan J and Angell C A 1994 *J. Phys. Chem.* **98** 13780
[115] Hayward J A, Finney J L, Daniel R M and Smith J C 2003 *Biophys. J.* **83** 679
[116] Demmel F, Doster W, Petry W and Schulte A 1997 *Eur. Biophys. J.* **26** 327
[117] Bizzarri A R and Cannistraro S 1997 *Phys. Lett.* A **236** 596
[118] Weissman M B 1988 *Rev. Mod. Phys.* **60** 537
[119] Bizzarri A R and Cannistraro S 1999 *Physica* A **267** 257
[120] Painter P, Mosher L and Rhoads C 1982 *Biopolymers* **21** 1469
[121] Giraud G, Karolin J and Wynne K 2003 *Biophys. J.* **85** 1903
[122] Martel P, Calmettes P and Hennion B 1991 *Biophys. J.* **59** 363
[123] Brown K, Erfurth S, Small E W and Peticolas W L 1972 *Proc. Natl Acad. Sci. USA* **69** 1467
[124] Genzel L, Keilmann F, Martin T P, Winterling G, Yacoby Y, Froelich H and Makinen M W 1976 *Biopolymers* **15** 219
[125] Sokolov A P, Kisliuk A, Soltwish M and Quitmann D 1992 *Phys. Rev. Lett.* **69** 1540
[126] Russina M, Mezei F, Lechner R, Loneville S and Urban B 2000 *Phys. Rev. Lett.* **84** 3630
[127] Elliott S R 1992 *Europhys. Lett.* **19** 201
[128] Buchenau U 1992 *Phil. Mag.* B **65** 303
[129] Zeller C and Pohl O 1971 *Phys. Rev.* B **4** 2029
[130] Bellissent-Funel M C, Teixeira J, Chen S H, Dorner B and Crespi H L 1989 *Biophys. J.* **56** 713
[131] Melchionna S and Desideri A 1999 *Phys. Rev.* E **60** 4664
[132] Tarek M and Tobias D J 1999 *J. Am. Chem. Soc.* **121** 9740
[133] Angell C A, Poole P H and Shao J 1994 *Nuovo Cimento* **16** 993
[134] Angell C A 1995 *Science* **267** 1924
[135] Venturini F, Gallo P, Ricci M A, Bizzarri A R and Cannistraro S 2001 *J. Chem. Phys.* **114** 10010
[136] Dellerue S, Petrescu A J, Smith J C and Bellissent-Funel M C 2001 *Biophys. J.* **81** 1666
[137] Onuchic J N and Wolynes P 1993 *J. Chem. Phys.* **98** 2218
[138] Canters G W and van der Kamp M 1992 *Curr. Biol.* **2** 859
[139] Pande V S and Onuchic J N 1997 *Phys. Rev. Lett.* **78** 146
[140] Leite V B P and Onuchic J N 1996 *J. Phys. Chem.* **100** 7680
[141] Mungikar A A and Forciniti D 2002 *Chem. Phys. Chem.* **2** 993
[142] Willner I, Geleg-Shbtai V, Katz E, Rau H K and Haehnel W 1999 *J. Am. Chem. Soc.* **121** 6455
[143] Gilardi G, Fantuzzi A and Sadeghi S J 2001 *Curr. Opin. Struct. Biol.* **11** 491
[144] Andolfi L, Bonanni B, Canters G W, Verbeet M Ph and Cannistraro S 2003 *Surf. Sci.* **530** 181
[145] Kraulis P J 1991 *J. Appl. Crystallogr.* **24** 946